

Multinucleon transfer in the reaction  $^{12}\text{C}(p, ^6\text{Li})^7\text{Be}$  at  $E_p = 40.3$  MeV

G. D'Erasmus and V. Variale

*Dipartimento di Fisica dell'Università di Bari and Istituto Nazionale di Fisica Nucleare, Sezione di Bari, Bari, Italy*

A. Pantaleo

*Istituto Nazionale di Fisica Nucleare, Sezione di Bari, Bari, Italy*

(Received 9 July 1984)

Direct and exchange one-step transfer mechanisms have been investigated for the reaction  $^{12}\text{C}(p, ^6\text{Li})^7\text{Be}$  at  $E_p = 40.3$  MeV. The role of the  $^6\text{Li} + ^6\text{Li}$  clustering configuration for  $^{12}\text{C}$  is underlined.

In this work the multinucleon one-step transfer mechanism in the reaction  $^{12}\text{C}(p, ^6\text{Li})^7\text{Be}$  is studied through the fragment angular distribution, to provide clustering information on  $^{12}\text{C}$ . Should, in fact, the reaction proceed through one-step mechanisms, the angular distributions would reflect the transfer of specific clusters. Only one other cross section measurement of the reaction  $^{12}\text{C}(p, ^6\text{Li})^7\text{Be}$  is found,<sup>1</sup> which discriminates the ground from the first excited state in the residual  $^7\text{Be}$ . Two different interpretations<sup>1,2</sup> have been given to these experimental results. The former<sup>1</sup> explains the angular distributions only by the direct  $^5\text{He}$  pickup and the latter<sup>2</sup> invokes both direct and exchange processes. It seemed worthwhile in this context to provide an independent experimental evidence and analytical approach.

The experiment was made at the Milan AVF cyclotron. The 40.3 MeV analyzed proton beam was focused onto  $60 \mu\text{g}/\text{cm}^2$  self-supporting carbon targets and fragment angular

distributions were measured with both energy and time of flight<sup>3</sup> to obtain the energy spectra for the various mass ejectiles. Good timing resolution was achieved employing two microchannel plate transmission time detectors.<sup>4</sup> The energy was measured by means of a surface barrier totally depleted silicon detector with an energy resolution of 200 keV mainly due to target thickness. The two-body reaction was completely identified from kinematics and  $Q$  values. More details concerning the experiment can be found in Refs. 3 and 4. Figure 1 shows a typical time of flight spectrum and Fig. 2 two energy spectra for the ejectiles with mass numbers 6 and 7 with clear peaks due to the double ground state (g.s.) transition and to the  $^6\text{Li}_{\text{g.s.}} + ^7\text{Be}_{1\text{exc}}$  transition. The cross sections are displayed in Figs. 3 and 4 where the forward angle pattern is typical of direct reactions. The phase difference in the oscillations of the g.s. and first excited state angular distributions is a sign of the importance of the separation of the two levels. A comparison of our results with the previous ones at 51.9 MeV (Ref. 1) shows a cross section increase with beam decreasing energy, as expected for one-step reactions. Enhanced cross sections at backward angles are also evident, usually explained in terms of the exchange effects in the pickup reaction. In fact, if  $^{12}\text{C}$  is thought of as a  $^5\text{He}$  plus a  $^7\text{Be}$ , the incident proton can directly pickup a  $^5\text{He}$  to form  $^6\text{Li}$ . The forward angle maximum reflects the small momentum change of the

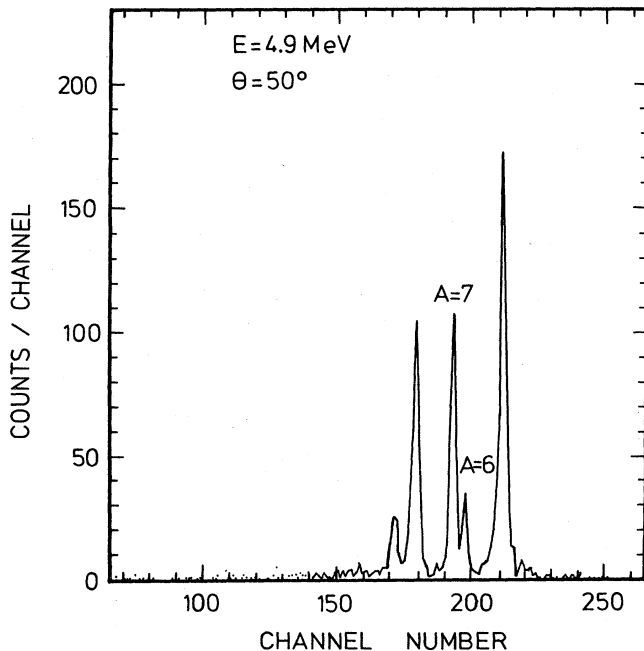


FIG. 1. Time of flight of different mass ejectiles with energy  $4.9 \pm 0.1$  MeV.

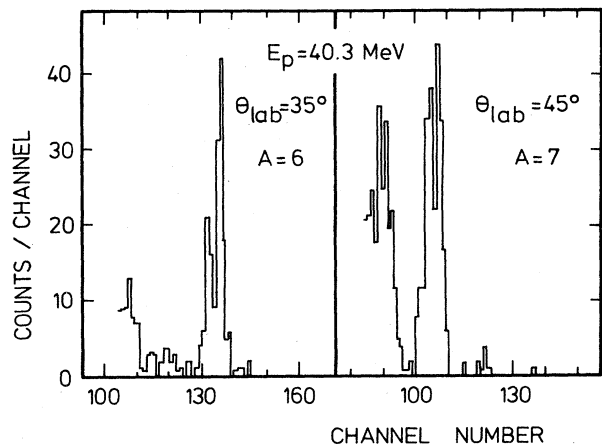


FIG. 2. Typical energy spectra for the masses  $A = 6$  and  $A = 7$ .

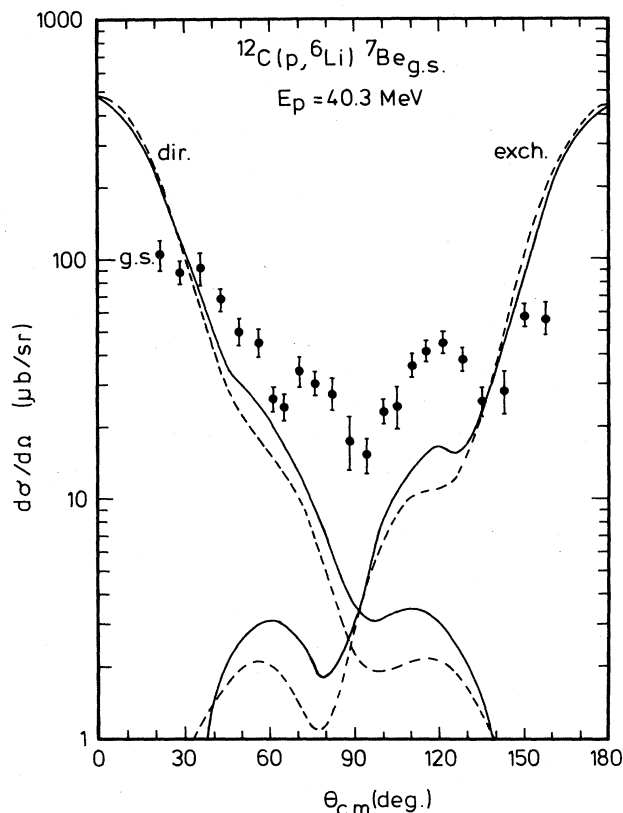


FIG. 3. Experimental differential cross section of the reaction  $^{12}\text{C}(p, ^6\text{Li})^7\text{Be}$  leading to the ground states of the final products. The dashed line is a DWBA calculation with the optical potentials of Table I(a), while the full line refers to the optical potentials of Table I(b). The spectroscopic factors (Table III) are the ones of Ref. 2.

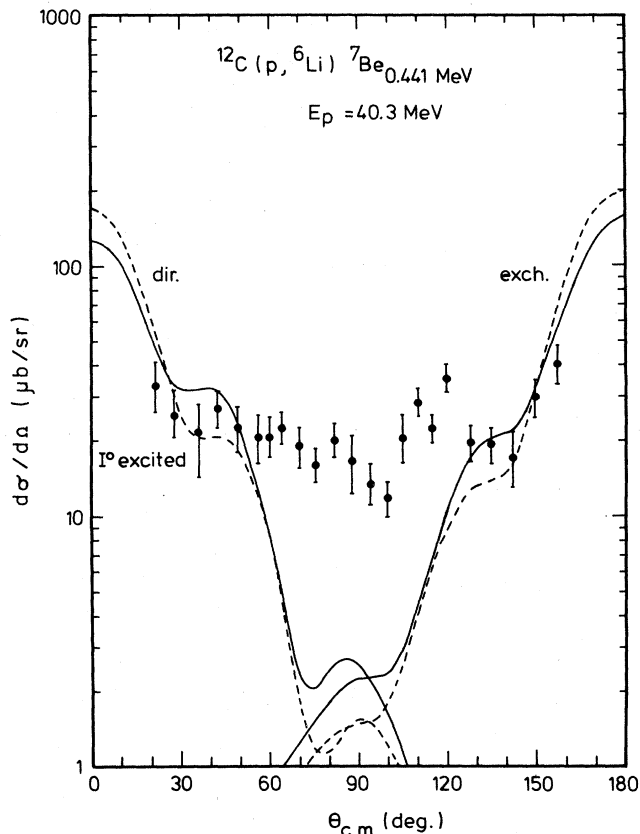


FIG. 4. Experimental differential cross section of the reaction  $^{12}\text{C}(p, ^6\text{Li})^7\text{Be}_{1\text{exc}}$  leading to the first excited state of  $^7\text{Be}$ . The lines have the same relation to the optical potentials as in Fig. 3. The spectroscopic factors are reported in Table IV.

incoming proton when this  $^6\text{Li}$  comes out in the forward direction. If instead  $^{12}\text{C}$  is considered as two  $^6\text{Li}$  clusters, the incident proton can pick up a  $^6\text{Li}$  and emerge mainly forward as  $^7\text{Be}$  while the residual  $^6\text{Li}$  recoils in the opposite direction (exchange process) enhancing the back angles cross section.

The results have been analyzed by means of distorted wave Born approximation (DWBA) calculations. The code DWUCK5 has been used, which accounts for the finite range of forces and for the recoil effects. The optical potential parameters used are reported in Tables I(a) and I(b). In

Table I(a) the parameters for the entrance channel have been adopted from a systematic<sup>5</sup> of proton scattering on medium-light nuclei, while those in Table I(b) come from a study<sup>6</sup> relative to only  $^{12}\text{C}$ . All the exit channel parameters have been searched for in a best fit to the measured cross sections, because of the lack of  $^6\text{Li} + ^7\text{Be}$  scattering data due to the short  $^7\text{Be}$  lifetime. Real depths were found smaller than the ones published<sup>7</sup> for  $^6\text{Li} + ^9\text{Be}$  up to 24.5 MeV.

The bound states of  $^{12}\text{C} \rightarrow ^7\text{Be} + ^5\text{He}$  and  $^6\text{Li} \rightarrow ^5\text{He} + p$  in the direct process and of  $^{12}\text{C} \rightarrow ^6\text{Li}(1) + ^6\text{Li}(2)$  and  $^7\text{Be} \rightarrow ^6\text{Li} + p$  in the exchange process were solved with the

TABLE I. Optical potentials. The entrance channel parameter come from (a) a systematic (Ref. 5) of proton scattering on medium-light nuclei and (b) a study (Ref. 6) relative to only  $^{12}\text{C}$ .

(a)	$V_R$ (MeV)	$r_R$ (fm)	$a_R$ (fm)	$W_V$ (MeV)	$W_S$ (MeV)	$r_W$ (fm)	$a_W$ (fm)	$r_c$ (fm)
$p + ^{12}\text{C}$	-45.3	1.064	0.623	0.00	4.0	1.2	0.6	1.2
$^6\text{Li} + ^7\text{Be}$	-69.6	1.18	0.81	0.00	15.53	2.5	0.9	2.0
(b)	$V_R$ (MeV)	$r_R$ (fm)	$a_R$ (fm)	$W_V$ (MeV)	$W_S$ (MeV)	$r_W$ (fm)	$a_W$ (fm)	$r_c$ (fm)
$p + ^{12}\text{C}$	-56.5	1.064	0.623	0.00	6.15	1.2	0.6	1.2
$^6\text{Li} + ^7\text{Be}$	-72.39	1.18	0.81	0.00	14.29	2.5	0.9	2.0

TABLE II. Bound state parameters:  $n$  is the number of nodes of the wave function and  $l$  is the relative motion angular momentum.

	$n$	$l$	$r_c$ (fm)	$V$ (MeV)	$r_0$ (fm)	$a_R$ (fm)	$E_B$ (MeV)
$^{12}\text{C} \rightarrow ^7\text{Be} + ^5\text{He}$	2	0	2.83	52.74	2.83	0.545	27.16
	1	2	2.83	51.63	2.83	0.545	27.16
$^6\text{Li} \rightarrow ^5\text{He} + \text{p}$	0	2	1.11	81.51	1.11	0.650	4.59
$^{12}\text{C} \rightarrow ^6\text{Li} + ^6\text{Li}$	2	1	2.98	53.73	2.98	0.545	28.17
	1	2	2.98	52.63	2.98	0.545	28.17
$^7\text{Be} \rightarrow ^6\text{Li} + \text{p}$	0	1	1.38	55.90	1.38	0.780	5.61

potential parameters in Table II (from Ref. 2), because different geometries proved to be connected to the depths preserving the volume integral of the potential, without big effects on the shape of the results. The spectroscopic amplitudes for the direct and exchange processes relative to the ground state of  $^7\text{Be}$  (Table III) come from the same calculation.<sup>2</sup>

A first approach, considering only the direct process and fitting to the experimental cross section the exit channel optical potentials, failed to reproduce the backward angle rise of the angular distribution. A similar failure of the simple direct process was tested in a search for different spectroscopic amplitudes, having fixed the potential parameters for the entrance channel as said above and for the exit channel to different reasonable guesses from the literature.<sup>1,2,7</sup>

Figure 3 shows the fit obtained for the double g.s. transition cross section by taking into account both the direct and exchange processes. In these calculations the spectroscopic amplitudes of Ref. 2 were adopted and the exit channel op-

tical potentials of Table I were obtained from the search (dashed and full lines for the different entrance channel potentials). With the same meaning of lines, in Fig. 4 the results are shown for the calculations relative to the  $^7\text{Be}$  first excited state transition. Here the optical potentials have been fixed to the same values of the g.s. transition, on account of the small  $Q$ -value difference, and the lacking spectroscopic amplitudes have been searched for in the best fit to the data, giving the results summarized in Table IV. Owing to the experimental uncertainties, only a small  $\chi^2$  difference favors the potentials of Table I(b) both in Figs. 3 and 4, while no simple suggestion can be given for the strong constructive interference needed at mid-angles between the direct and exchange processes.

As a conclusion, our results underline the role of the exchange process in the mechanism of the one-step multinucleon transfer reaction  $^{12}\text{C}(p, ^6\text{Li})^7\text{Be}$ . From this, a non-negligible  $^6\text{Li}$  clustering probability can be deduced for  $^{12}\text{C}$ , in addition to a clear  $^5\text{He} + ^7\text{Be}$  configuration.

TABLE III. Spectroscopic amplitudes relative to the  $^7\text{Be}$  in the g.s.: (a)  $S_{^{12}\text{C}(^5\text{He}, ^7\text{Be})}$  for the g.s. of  $^{12}\text{C}$  and  $S_{^6\text{Li}(p, ^5\text{He})}$  for the g.s.  $^6\text{Li}$  (direct transfer); (b)  $S_{^{12}\text{C}(^6\text{Li}, ^6\text{Li})}$  for the g.s. of  $^{12}\text{C}$  and  $S_{^7\text{Be}(p, ^6\text{Li})}$  for the g.s. of  $^7\text{Be}$  (exchange transfer);  $J_1$  is the core spin and  $j_1 = J_1 + 1_1$ ,  $j_2 = J_1 + 1_2$  are the total angular momenta of the configurations here considered.

Core $^5\text{He}$		$^{12}\text{C}(gnd) \rightarrow ^5\text{He} + ^7\text{Be}(gnd)$				$^6\text{Li}(gnd) \rightarrow ^5\text{He} + \text{p}$	
$J_1$	$l_1$	$J_1$	$S_{^{12}\text{C}(^5\text{He}, ^7\text{Be})}$	$i_2$	$J_2$	$S_{^6\text{Li}(p, ^5\text{He})}$	
(a) $\frac{3}{2}$	0	$\frac{3}{2}$	-0.7930	1	$\frac{1}{2}$	-0.5963	
				1	$\frac{3}{2}$	0.6667	
	2	$\frac{3}{2}$	0.5245	1	$\frac{1}{2}$	-0.5963	
				1	$\frac{3}{2}$	0.6667	
$\frac{1}{2}$	2	$\frac{3}{2}$	-0.5245	1	$\frac{1}{2}$	-0.2108	
				1	$\frac{3}{2}$	0.5963	
Core $^6\text{Li}$		$^{12}\text{C}(gnd) \rightarrow ^6\text{Li} + ^6\text{Li}(gnd)$				$^7\text{Be}(gnd) \rightarrow ^6\text{Li} + \text{p}$	
$J_1$	$l_1$	$J_1$	$S_{^{12}\text{C}(^6\text{Li}, ^6\text{Li})}$	$i_2$	$J_2$	$S_{^7\text{Be}(p, ^6\text{Li})}$	
(b)	0	1	-0.8381	1	1	-0.6573	
				1	2	-0.7349	
	2	1	0.5355	1	2	-0.7349	

TABLE IV. Spectroscopic amplitudes relative to the  ${}^7\text{Be}$  in the first excited state: (a)  $S_{12\text{C}({}^5\text{He}, {}^7\text{Be}_{1\text{exc}})}$  for the g.s. of  ${}^{12}\text{C}$  and  $S_{6\text{Li}(p, {}^5\text{He})}$  for the g.s. of  ${}^6\text{Li}$  (direct transfer); (b)  $S_{12\text{C}({}^6\text{Li}, {}^6\text{Li})}$  for the g.s. of  ${}^{12}\text{C}$  and  $S_{7\text{Be}_{1\text{exc}}(p, {}^6\text{Li})}$  for the first excited state of the  ${}^7\text{Be}$  (exchange transfer); same meaning of  $J_1$  and  $j_{1,2}$  as in Table III.

Core ${}^5\text{He}$		${}^{12}\text{C}(gnd) \rightarrow {}^5\text{He} + {}^7\text{Be}(1\text{exc})$			${}^6\text{Li}(gnd) \rightarrow {}^5\text{He} + p$		
$J_1$	$l_1$	$j_1$	$S_{12\text{C}({}^5\text{He}, {}^7\text{Be}_{1\text{exc}})}$	$l_2$	$j_2$	$S_{6\text{Li}(p, {}^5\text{He})}$	
$\frac{3}{2}$	2	$\frac{1}{2}$	0.3578	1	$\frac{3}{2}$	-0.1187	
				1	$\frac{1}{2}$	0.8404	
(a) $\frac{1}{2}$	0	$\frac{1}{2}$	0.9894	1	$\frac{1}{2}$	-0.3817	
Core ${}^6\text{Li}$		${}^{12}\text{C}(gnd) \rightarrow {}^6\text{Li} + {}^6\text{Li}(gnd)$			${}^7\text{Be}(1\text{exc}) \rightarrow {}^6\text{Li} + p$		
$J_1$	$l_1$	$j_1$	$S_{12\text{C}({}^6\text{Li}, {}^6\text{Li})}$	$l_2$	$j_2$	$S_{7\text{Be}_{1\text{exc}}({}^6\text{Li}, p)}$	
	0	1	0.8526	1	1	0.1862	
(b)				1	0	0.4867	
	2	1	0.2694	1	1	-0.0883	
				1	0	0.9169	

<sup>1</sup>S. Kato, S. Kubono, T. Yamaya, H. Endo, K. Takimoto, K. Fusii, J. Shimizu, N. Takahashi, Y. Iwasaki, and J. Kasagi, Phys. Lett. **62B**, 153 (1976).

<sup>2</sup>Y. Kudo, T. Honda, and H. Horie, Prog. Theor. Phys. **59**, 101 (1978).

<sup>3</sup>R. De Leo, G. D'Erasmus, A. Pantaleo, V. Paticchio, V. Variale, S. Micheletti, and M. Pignanelli, report INFN/BE-83/9, 1983.

<sup>4</sup>G. D'Erasmus, V. Paticchio, and A. Pantaleo, Nucl. Instrum. Methods (in press).

<sup>5</sup>F. Fabrici, S. Micheletti, M. Pignanelli, F. G. Resmini, R. De Leo, G. D'Erasmus, A. Pantaleo, J. L. Escudié, and A. Tarrats, Phys. Rev. C **21**, 830 (1980).

<sup>6</sup>R. De Leo, G. D'Erasmus, F. Ferrero, A. Pantaleo, and M. Pignanelli, Nucl. Phys. **A254**, 156 (1975).

<sup>7</sup>J. Cook, Nucl. Phys. **A375**, 238 (1982), and references therein; J. E. Poling, E. Norbeck, and R. R. Carlson Phys. Rev. C **13**, 648 (1976).